

## Applications of Power Ultrasonics in Engineering

M. Lucas<sup>1,a</sup>, A. Cardoni<sup>1,b</sup>, E. McCulloch<sup>1</sup>, G. Hunter<sup>1</sup>, A. MacBeath<sup>1</sup>

<sup>1</sup>The University of Glasgow, Dept Mechanical Engineering, Glasgow G12 8QQ, UK

<sup>a</sup>m.lucas@mech.gla.ac.uk, <sup>b</sup>a.cardoni@mech.gla.ac.uk

**Keywords:** Power ultrasonics, ultrasonic cutting, ultrasonic cavitation, finite element modelling

**Abstract.** Applications of power ultrasonics in engineering are growing and now encompass a wide variety of industrial processes and medical procedures. In the field of power ultrasonics, ultrasonic vibrations are used to effect a physical change in a medium. However, the mechanism by which a process can benefit from power ultrasonics is not common for all applications and can include one or more of such diverse mechanisms as acoustic cavitation, heating, microfracture, surface agitation and chemical reactions. This paper presents two applications of power ultrasonics involving some of these different characteristics by concentrating on two case studies involving material failure (ultrasonic cutting) and acoustic cavitation (bacterial inactivation).

### Introduction

Power ultrasonics is a branch of ultrasonics that uses the vibrational energy of a device oscillating at an ultrasonic frequency in order to effect a physical change in a medium. This differentiates power ultrasonics from diagnostic (or imaging) ultrasound. The frequencies used in power ultrasonic applications are usually in the low ultrasonic range, of 20-100 kHz, and the power requirements, usually tens of watts to several kiloWatts, are usually significantly higher than those required in other ultrasonic applications, although these boundaries are becoming increasingly blurred.

The ability to create mechanical ultrasonic vibrations came with the discovery of the piezoelectric effect by Pierre and Jacques Curie in 1881 and the first practical application came during the First World War with the development of sonar for the detection of submarines. Since then its use as an imaging tool has been extended to medical diagnostics as well as to non-destructive testing of materials and structures. The destructive power of ultrasound was first reported by Langevin who observed the killing of fish subjected to a beam of ultrasound. This was to be the start of the field of power ultrasonics [1]. In 1926, Loomis and Wood extended Langevin's work to explain the chemical and biological effects of high power ultrasound [2] and were the first researchers to create an ultrasonic horn by drawing a glass tube to a tapered point to concentrate the ultrasonic energy. In the 1950's the development of efficient transducers and the design of tapered half-wavelength ultrasonic horns for vibration amplification [3] led to many new ultrasonic industrial and clinical processes. For example, in medicine and dentistry power ultrasonics applications include destruction of tumours and kidney stones, cutting tissue in surgical procedures, dental surgery and descaling and cleaning of teeth. In the food industry alone power ultrasonic applications include food preservation, degassing foams, filtration, drying and cutting of foodstuffs [4,5]. Three of the most widely used and well known industrial applications are ultrasonic cleaning, plastic welding and ultrasonic machining (USM).

Ultrasonic cleaning utilises the cavitation effect. Oscillating bubbles collapsing at the surfaces of a component to be cleaned cause extremely high localised temperatures and pressures which result in breakdown of oxide layers, disruption and removal of contaminants and inactivation of bacterial cells [6].

Plastic welding is fast, clean and easily automated and is commonly used in the manufacture of plastic toys, in sealing plastic bottle caps and in joining thermoplastic components. The oscillatory

movement of the horn produces a highly localised temperature rise at the interface between the horn and work-piece causing the work-piece to melt locally at the weld zone, with little heat transfer to the bulk material [7].

In ultrasonic machining an abrasive slurry consisting of water or oil with particles of silicon carbide suspended in solution are fed to the interface between the ultrasonic tool and work-piece. The ultrasonic vibrations force the abrasive particles in the slurry into the work-piece resulting in micro cracking and material removal [8].

What is clear from these few industrial examples is that the common element is an ultrasonic transducer and horn configuration that delivers vibrational energy either directly to a work-piece or via an intermediate load medium. There is then a wide range of destructive effects, caused by the delivery of this vibrational energy, that can be harnessed to extract significant benefits from a diverse range of industrial processes. In this paper, two very different applications are discussed: ultrasonic cutting, which can be considered as a controlled material failure process along a cut line; and bacterial inactivation, which occurs as a result of generating an acoustic cavitation field in a fluid.

### Ultrasonic Cutting

**Cutting systems.** Ultrasonic cutting systems were largely introduced in the food industry in the 1990's to allow high quality cuts with minimal product waste. Large volumes of food product can be cut under automated conditions in either a batch or continuous configuration using ultrasonic cutting knives in either a slicing or guillotining configuration. Advantages of using ultrasonically vibrating cutting blades include improved cut quality, especially of brittle products, reduced cut debris, self cleaning blades and longer tool life. Figure 1 shows three ultrasonic cutting systems from Branson Ultrasonics and Dukane, (a) and (b) showing blades using a guillotine configuration and (c) a multiple blade slicing configuration.



Fig. 1: Ultrasonic cutting in (a), (b) guillotine orientation and (c) slicing orientation [9,10]

**Stress considerations.** In each system the cutting blade is a multiple of the tuned half-wavelength at the operating frequency, which is usually between 20 and 40 kHz. In order to cut effectively, the blade cutting edge must be thin. By creating a blade that is thicker at the end in contact with the transducer, and reducing its cross-sectional area to create the cutting tip, as shown for example in Figure 2, amplitude gain is designed into the blade and sufficient ultrasonic amplitude can be excited at the cutting edge. As a consequence, blades can suffer breakages due to high stress and must be very carefully designed to produce geometries that can provide high ultrasonic amplitude within stress limits.

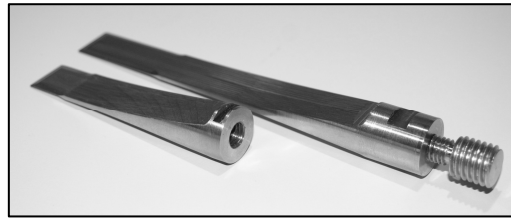


Fig. 2: Two half-wavelength ultrasonic cutting blades tuned to 20 kHz and 35 kHz.

The location and magnitude of the maximum stress and the vibration displacement can be calculated from finite element models of the cutting blade. Where the vibration node coincides with location of the maximum stress, as for the blade shown in Figure 3a, stress will be maximised and therefore one strategy to reduce stress in blades with high amplitude gain, is to design blade geometries that locate the vibration node away from the maximum stress location. The blades shown in Figure 2 have successfully adopted this strategy in the design of their profile.

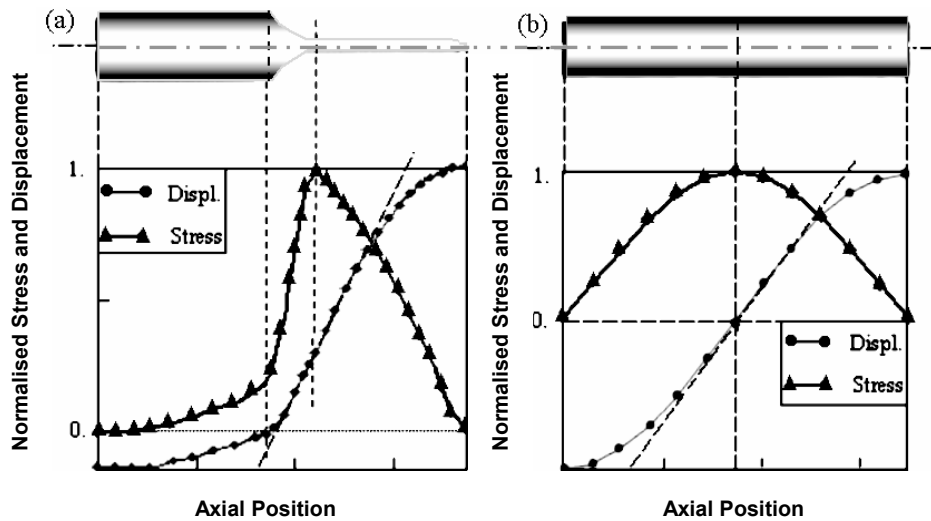


Fig. 3: Normalised stress and vibration displacement of (a) tuned cutting blade and (b) bar horn

**Dynamics characterisation.** Another consequence of requiring thin blades to cut effectively is that ultrasonic cutting systems suffer from problems associated with modal interactions [11]. Combination resonances are a common feature of the dynamic response of systems driven in longitudinal resonance and, for ultrasonic devices, multiple tuned-component systems with complex geometries are particularly prone to stress failures due to such modal interactions. Modal interactions can occur if special relationships exist between one or more modal frequencies and the excitation frequency. The type of modal interactions that can occur depends on the nature of the excitation and on the system nonlinearity [12].

An autoparametric system is one in which the forced response of the primary part of the system, possibly a single forced mode, acts as a parametric excitation on the secondary part, either as a principal parametric resonance involving one mode or a combination resonance involving multiple modes. The net effect is a two-way interaction between the two parts for which overall steady-states are possible. The effects of parametric excitation are such that very large responses may be generated in a plane perpendicular to that of the excitation, provided that certain relationships exist between the excitation frequency and the frequency of the excited internal mode or modes. In practice, for ultrasonic devices, the modal frequency relationships most often measured in systems exhibiting modal interactions are: a modal frequency is approximately equal to half the tuned excitation frequency, called a principal parametric resonance where  $\Omega/2 \approx \omega_1$ ; the sum of two modal

frequencies is approximately equal to the tuned excitation frequency, called a combination resonance or three-mode interaction where  $\Omega \approx \omega_2 + \omega_3$ .  $\Omega$  is the external excitation frequency (and tuned longitudinal mode resonant frequency of the system), and  $\omega_1, \omega_2, \omega_3$  are three internal modal frequencies.

As in the theoretical models, the modal interaction manifests itself as the excitation of large responses in flexural and torsional modes, in a plane perpendicular to the excitation direction, at frequencies lower than the excitation frequency. The responses are easily detected in a measurement of the response spectrum when the device is being driven at the tuned frequency and can be readily heard at their audible frequencies.

In Figure 4 the response characteristics of a three-blade cutting device featuring a double-slotted block horn are investigated. A frequency response function (FRF) measured from a position on one of the outer blades in the 0-50 kHz range is shown in Figure 4(b). The response spectrum, measured when the device is driven only at the tuned longitudinal mode operating frequency at 35.5 kHz, shows evidence of an internal coupling of the externally excited mode with two flexural modes at 10.8 kHz and 24.5 kHz, as illustrated in Figure 4(c). The measurement is characteristic of a three-mode combination resonance, where a frequency relationship  $\Omega \approx \omega_2 + \omega_3$  is satisfied.

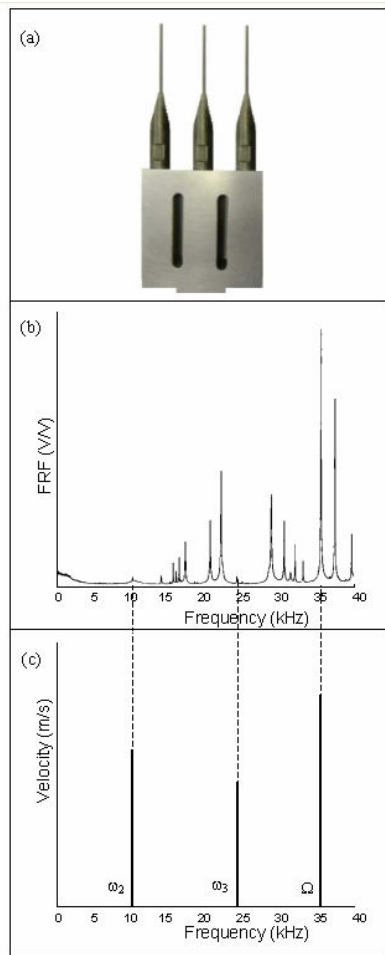


Fig. 4: (a) Cutting device, (b) FRF, (c) frequency response for system driven at 35.5 kHz in tuned longitudinal mode

The consequence of modal interactions is that energy leaks from the tuned longitudinal mode, required for effective cutting, into untuned flexural modes, causing poor cutting performance, high stresses in the blades and unacceptable audible frequency noise. Further characterisation of the modal interaction allows a threshold to be identified under which excitation levels will not excite this phenomena. However, in practical applications, requiring high ultrasonic amplitudes for

cutting, the design of cutting systems should try to keep the number of modes as low as possible by simplifying the geometry wherever possible and identification, via finite element modelling, of modes likely to satisfy the special relationships for modal interactions, should be identified at the design stage.

**Finite element modelling of ultrasonic cutting.** Finite element (FE) models of ultrasonic cutting have been developed in order to provide a vehicle for designing cutting blades more specifically focussed on the material to be cut. The FE models allow parametric studies of the effects of cutting parameters such as cutting speed, applied load, ultrasonic amplitude and frequency, without the need for extensive experiments. However, the accuracy of the FE model relies critically on the material model. For food products, the materials to be cut are often highly complex and difficult to characterise. A considerable research effort has therefore been made to define material models for some common food products. An example is toffee, which is highly temperature and strain rate dependent and has been tested in tension and compression in order to characterise stress-strain data which can be input into the FE model. The tension test specimens are shown in Figure 5 and the resulting measured stress-stain data at different test temperatures and strain rates (or cross-head velocities) is shown in Figure 6.



Fig. 5: Tensile test specimens of toffee in specially designed grips

The fully coupled thermal-stress 3D FE simulation developed for ultrasonic cutting uses element erosion to define material failure within ABAQUS [13]. The model utilises the shear failure option for each stress-strain curve at every test temperature and strain rate defined in the model by the user. ABAQUS defines the shear failure of the material as a number between 0 and 1 at each temperature and strain rate. 0 defines the stress at the yield point or where plastic strain is 0, and 1 is the stress at maximum plastic strain defined by the user in the stress-strain curve in the material representation. When the equivalent plastic strain in the material reaches the predetermined shear failure value, usually at the break point of the material, the element is eroded, which simply means that the material properties ramp down to 0. The adaptive mesh option is also used automatically in the element erosion model to allow the nodal coordinates of highly deformed elements that have not yet eroded, to be automatically adjusted to ensure the model remains within convergence limits until the analysis has ended or the element has been eroded from the analysis. The excited ultrasonic blade simply destroys the elements within its path as it translates through the material. A result of the FE simulation showing contours of temperature distribution in the cutting blade is shown in Figure 7.

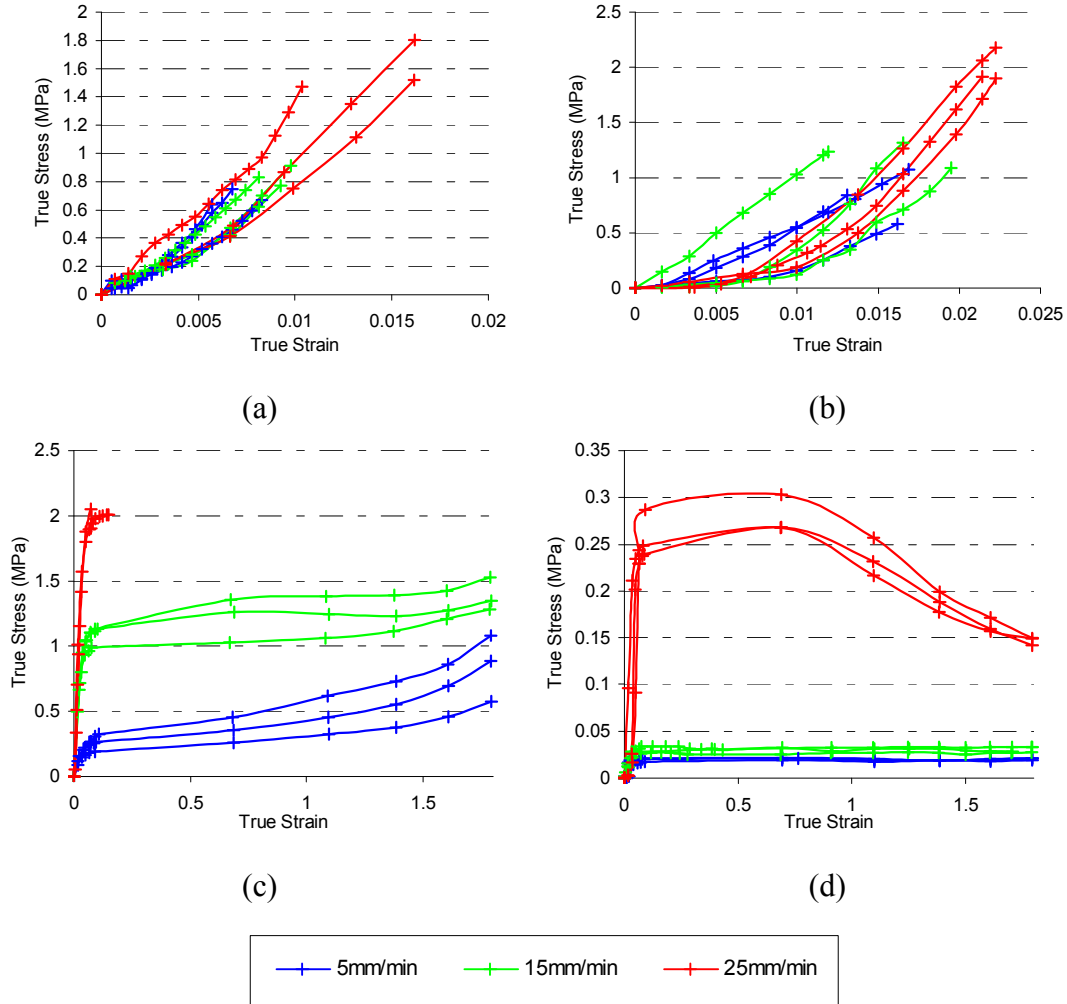


Fig. 6: Experimental tensile test data for toffee at (a) 20°C (b) 25°C (c) 30°C (d) 35°C

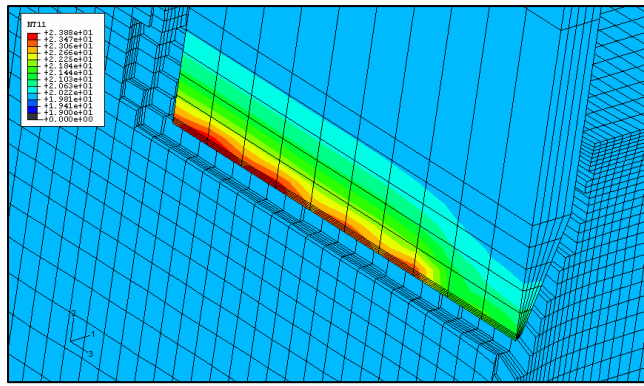


Fig. 7: FE model of ultrasonic cutting illustrating the temperature in the blade

### Ultrasonic Bacterial Inactivation

**Introduction.** Biologically, ultrasound is safe in low power applications, however as the power is increased some interesting effects take place. At high power, ultrasonic vibrations can cause cavitation, a process whereby bubbles in the fluid are formed and subsequently collapse violently. Cavitation has found many and varied uses in engineering, physical science (most notably in chemistry), medicine and dentistry. Common applications of cavitation are for cleaning, homogenisation, sonochemistry, lithotripsy, and cell disruption.

The use of cavitation in nature to stun or kill prey has been recorded in the closure of shrimp claws. It has also been suggested that dolphins can focus their ultrasound to stun or kill their prey. In the case of microorganisms, the mechanism of cell death is through the exposure to high pressure shock waves developed upon the collapse of a cavitation bubble.

Since Langevin's initial studies, there have been some attempts to scale up and commercialise systems using ultrasound for the bacterial inactivation of waste water, dairy products and fruit juices. The majority of the systems currently used at the laboratory scale are based on a longitudinally vibrating probe device such as the one shown in Fig. 8.



Fig. 8: A 20 kHz ultrasonic probe device

This type of system is ideal for treating small volumes of fluid in a batch process and has been used for many years. In the processing of liquids under no flow conditions using ultrasound there has been very little innovation from the probe system. This is probably due to the efficiency of the system at the laboratory scale. However, due to the nature of the cavitation field generated by these devices they are not particularly suitable when there is a continuous flow of fluid to be treated. There are also many processes where it would be much safer and more convenient not to remove fluid in batches during the process in order to treat it for bacterial inactivation.

**Radial mode ultrasonic horns.** Research has concentrated on designing a radial mode ultrasonic horn which can be accommodated in-line in fluid processing for ultrasonic bacterial inactivation. The ultrasonic transducer is attached to a tuned thick cylinder which vibrates in the R0 mode shape, where the circumference expands and contracts uniformly. The cylinder is attached to two tuned thin pipes which have structural mounting flanges at the vibration nodes so that vibrational energy is not lost to the attached structure. A representation in the form of a finite element mesh is shown in Figure 9. Another radial mode horn, tuned to the third radial harmonic mode frequency, the R3 mode, was also designed to investigate how the mode shape affected the cavitating region in the fluid cavity and resulting bacterial inactivation.

**Finite element models.** FE models were created using ABAQUS to simulate the acoustic pressure field created by an ultrasonic probe and ultrasonic radial horns tuned to two different radial modes of vibration; R0 and R3. The water in the fluid cavity was modelled using acoustic elements, which allow the pressure to be calculated from a fluid under stress. This type of analysis has limitations. Firstly, it is only valid up to the point of cavitation inception and is therefore only used to indicate where cavitation is most likely to occur and not to model the cavitating region. The second limitation is that the fluid cavity must be considered as stationary.

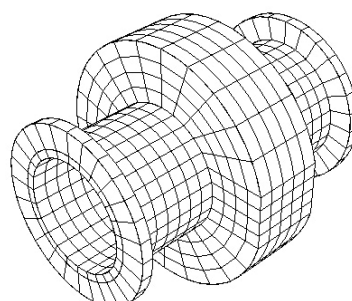


Fig. 9: Finite element model of the radial mode ultrasonic horn

**Visualisation of the cavitation field.** Visualisation of the cavitation field provides a means of characterising the acoustic cavitation field. The bubble size and size of the fluid cavity allows photographs to be taken which indicate the size and shape of the cavitation field generated. Further, the strength of the cavitation field at specific points within the fluid can be estimated using aluminium foil. Also, cavitation bubble collapse causes the release of free radicals which are highly reactive. The reaction between these radicals and luminol solution gives rise to an emission of blue light which can be used to indicate areas undergoing cavitation and provides a further visualisation of the cavitation field.

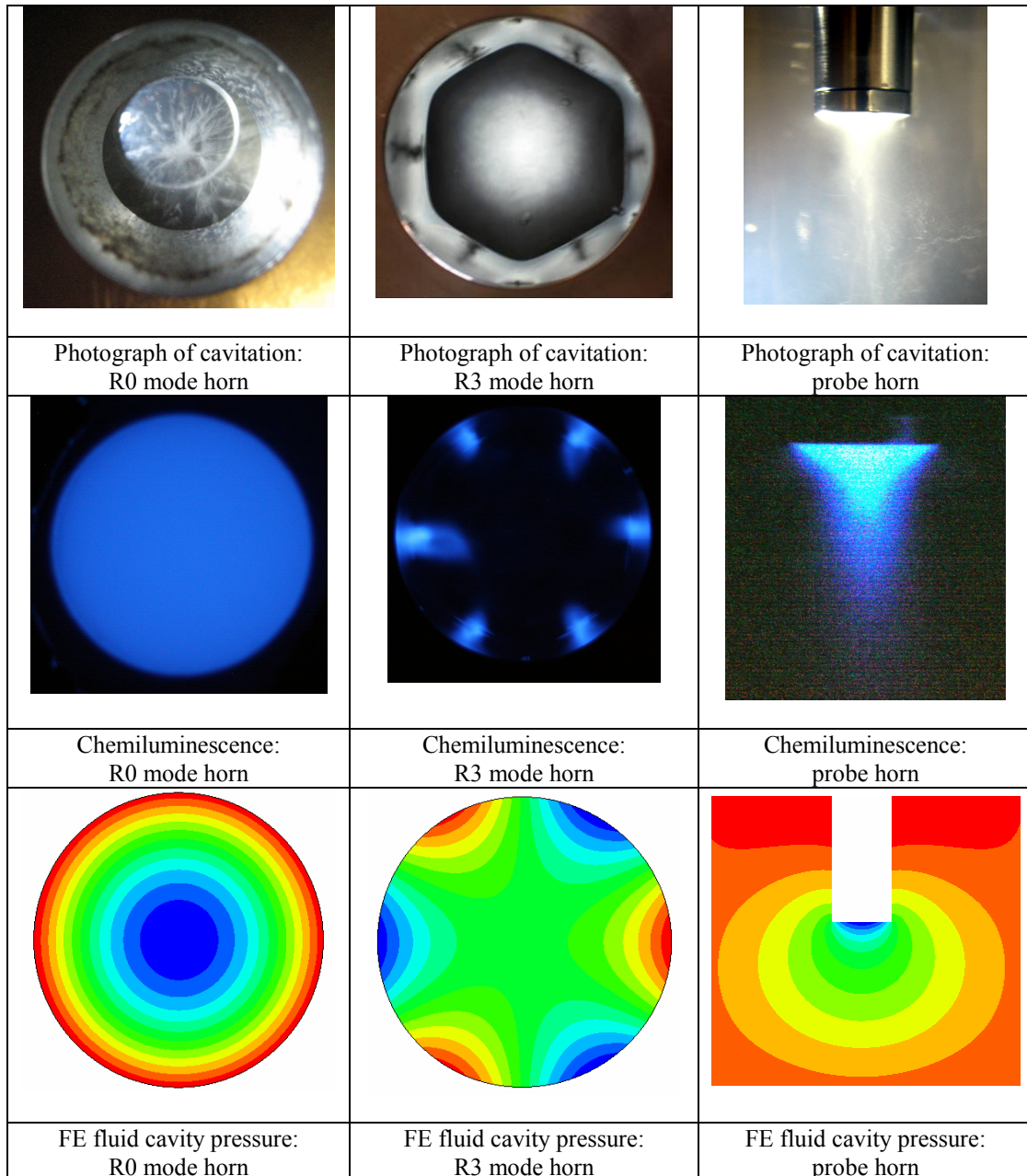


Fig. 10: Comparison of cavitation field visualisations using photographs and chemiluminescence with FE predictions of the acoustic pressure in the fluid cavity.

Figure 10 shows the results from the visualisation study. It can be observed from the photographs in the first row that the R0 mode horn creates a focussed bubble field in the centre of the fluid cavity away from the vibrating face. The R3 mode horn produces a hexagonal structure of fluid in the centre which is not undergoing cavitation, the position of the vertices of this hexagon relate to the nodes of the mode of vibration. The fluid outwith this hexagon is cavitating, with stronger cavitation occurring at the anti-nodes. The probe horn creates a conical cavitation field close to the vibrating tip.

These patterns of cavitation activity are confirmed by the chemiluminescence of luminol, shown in the second row of Figure 10. The R0 mode radial horn produces a uniform light output throughout the fluid in the cavity, indicating that there is cavitation throughout the fluid volume and not only at the centre, whilst the R3 radial horn produces six distinct light points known to be at the anti-nodes of the horn mode shape. The probe device creates a conical blue volume in the fluid.

The third row shows the predicted pressure fields in the fluid cavity for all three devices from the FE models. It can be seen that the predicted pressure fields correlate well with the experimentally observed cavitation fields using photographs and chemiluminescence. In the case of the R0 and R3 radial horns there is good correlation between the locations of the observed cavitation fields and the FE predicted locations of high pressure. However, the results from the probe horn study indicate that although the finite element model predicts high pressure at the probe tip, the pressure field close to the tip is dome shaped rather than cone shaped as observed in experiments. It is likely that the formation of a cone shaped bubble field lies in the primary Bjerknes forces and high pressure zones can actually repel bubbles, thus it is not surprising that the predicted pressure field does not exhibit a cone like structure. The primary Bjerknes forces are radiation forces caused by bubbles being acted upon by a sound field and are the most significant force after buoyancy.

**Bacterial inactivation results.** Figure 11 shows the survival of *E. coli* K12 during treatments with the radial horn (R0) and probe horn for the same power density of 12.57 W/cm<sup>3</sup>. It can be seen that the radial horn, operating at a considerably lower ultrasonic amplitude than the probe device (5 µm compared to 100 µm), produces improved bacterial inactivation. In fact, the radial horn provides an additional 0.3 log reduction in viable bacterial cells after exposure for 5 minutes. It is expected that this is as a result of the focussing of the cavitation field provided by the radial horn. It can also be observed that using the radial horn operating at a higher power density, of 18.86 W/cm<sup>3</sup>, results in an additional 0.5 log reduction in bacterial numbers [14].

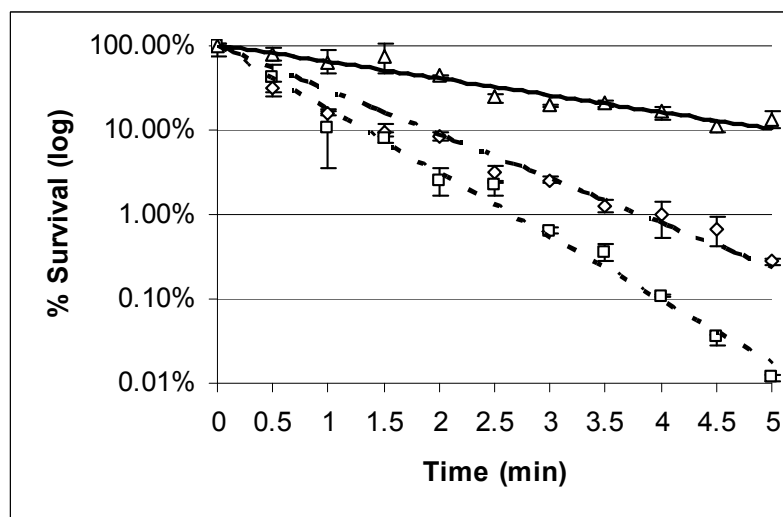


Fig.11: Bacterial inactivation (*E. coli* K12) as a function of exposure time for: □ R0 horn 18.86 W/cm<sup>3</sup>, ◇ R0 horn 12.57 W/cm<sup>3</sup>, Δ probe horn 12.57 W/cm<sup>3</sup>.

## Conclusions

This paper has highlighted some of the very different mechanisms by which power ultrasonics can provide benefits to industrial processes and has indicated some of the acoustics, vibration response, materials and fluid behaviour issues that arise in two illustrative example applications of ultrasonic cutting and ultrasonic bacterial inactivation.

## References

- [1] K.F. Graff, A History of Ultrasonics, Chapter 1 of Physical Acoustics, Vol. 15, Eds. Mason and Thurston, Academic Press (1981).
- [2] R.W. Wood, A.L. Loomis, The Physical and Biological Effects of High Frequency Sound Waves of High Intensity, Philosophy Magazine, Vol. 4 (1927).
- [3] L.G. Merkulov, Theory of Ultrasonic Concentrators, Soviet Physical Acoustics, Vol. 3, 230-238 (1957).
- [4] T.J. Mason, Power Ultrasound in Food Processing – The Way Forward, In: Ultrasound in Food Processing, Eds. M.J.W. Povey, T.J. Mason, Blackie Academic, 105-125 (1998).
- [5] J.A. Gallego-Juarez, Some Applications of Air-Borne Power Ultrasound to Food Processing, In: Ultrasound in Food Processing, Eds. M.J.W. Povey, T.J. Mason, Blackie Academic, 127-143 (1998).
- [6] B. Lambert, Ultrasonic Cleaning Aids to Production, Engineering (London), Vol. 219, 329-331 (1979).
- [7] A. Shoh, Welding of Thermoplastics by Ultrasound, Ultrasonics, 209-217, (1976).
- [8] E.A. Nepiras, Report on Ultrasonic Machining, Metalworking Production, Vol. 100, 1283-8 (1956).
- [9] [www.branson-plasticsjoin.com/applications\\_food.asp](http://www.branson-plasticsjoin.com/applications_food.asp)
- [10] [www.dukcorp.com/us/products/food/whatisFP.htm](http://www.dukcorp.com/us/products/food/whatisFP.htm)
- [11] A. Cardoni, F.C.N. Lim, M. Lucas, M.P. Cartmell, Characterising Modal Interactions in an Ultrasonic Cutting System, Forum Acusticum paper ULT-02-003-IP, Seville, Spain (2002).
- [12] M.P. Cartmell, Introduction to Linear, Parametric and Nonlinear Vibrations, Chapman and Hall World Publishing Corporation, UK (1990).
- [13] E. McCulloch, A. MacBeath, M. Lucas, A Finite Element Model for Ultrasonic Cutting of Toffee, Proc. Modern Practice in Stress and Vibration Analysis, Applied Mechanics and Materials, Vol. 5-6, 519-526 (2006).
- [14] G. Hunter, M. Lucas, I. Watson, R. Parton, A Radial Mode Ultrasonic Horn for the Inactivation of Escherichia coli K12, Ultrasonics Sonochemistry, Vol. 15, 101-109 (2007).